

Addressing The False Negative Problem of Deep Learning MRI Reconstruction Models by Adversarial Attacks and Robust Training

Paper #28



Kaiyang Cheng*, Francesco Calivà*, Rutwik Shah, Misung Han,
Sharmila Majumdar, Valentina Pedoia

Disclosure

I have no financial interests or relationships to disclose with regard to the subject matter of this presentation.

Funding source

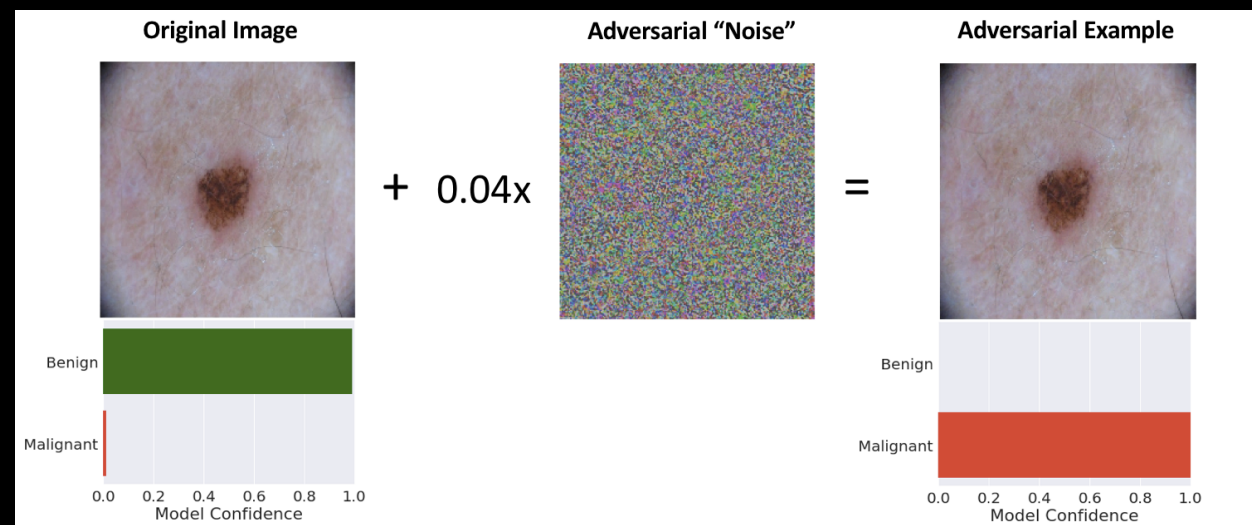
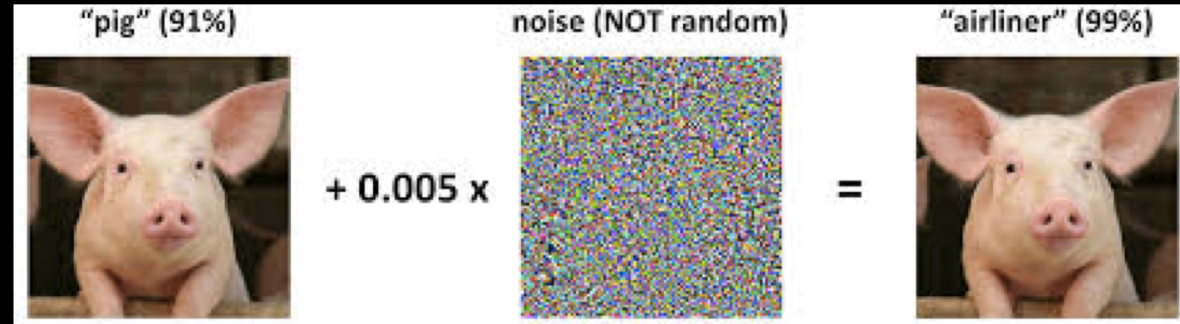
This project was supported by R00AR070902 (VP), R61AR073552 (SM/VP) from the National Institute of Arthritis and Musculoskeletal and Skin Diseases, National Institutes of Health, (NIH-NIAMS).



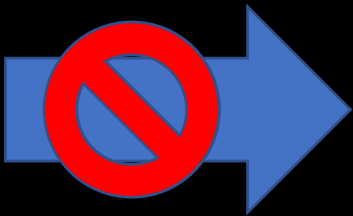
Outline

- *Motivation*
- *False negative problem in accelerated MRI reconstruction*
- *Adversarial examples*
- *FNAF attack*
- *Adversarial robustness training*
- *FNAF robust training*
- *Experimental results*
- *Conclusions*

Adversarial Examples in Medical Imaging Analysis



Adversarial Examples in Medical Imaging Analysis



IID Machine Learning vs Adversarial Machine Learning

$$\mathbb{E}_{(x,y) \sim D} [L(x, y, \theta)]$$

IID:

Average Case

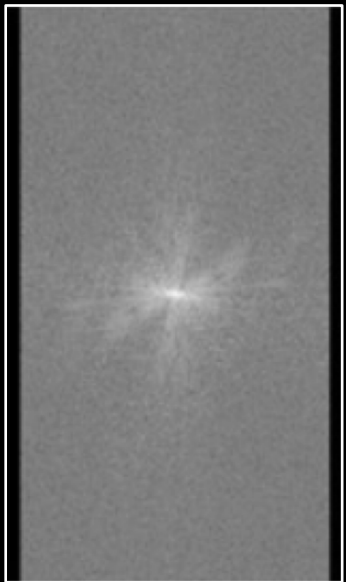
$$\mathbb{E}_{(x,y) \sim D} [\max_{\delta \in S} L(\theta, x + \delta, y)]$$

Adversarial:

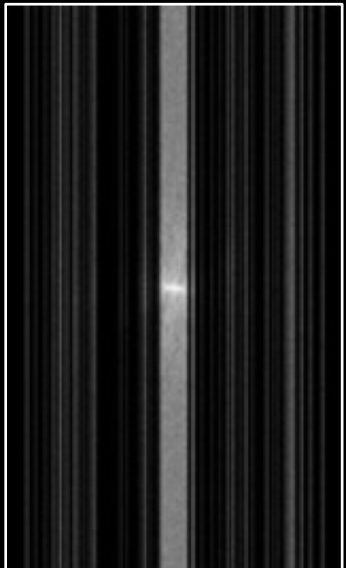
Worst Case

Accelerated MRI Reconstruction

Fully-sampled
k-space



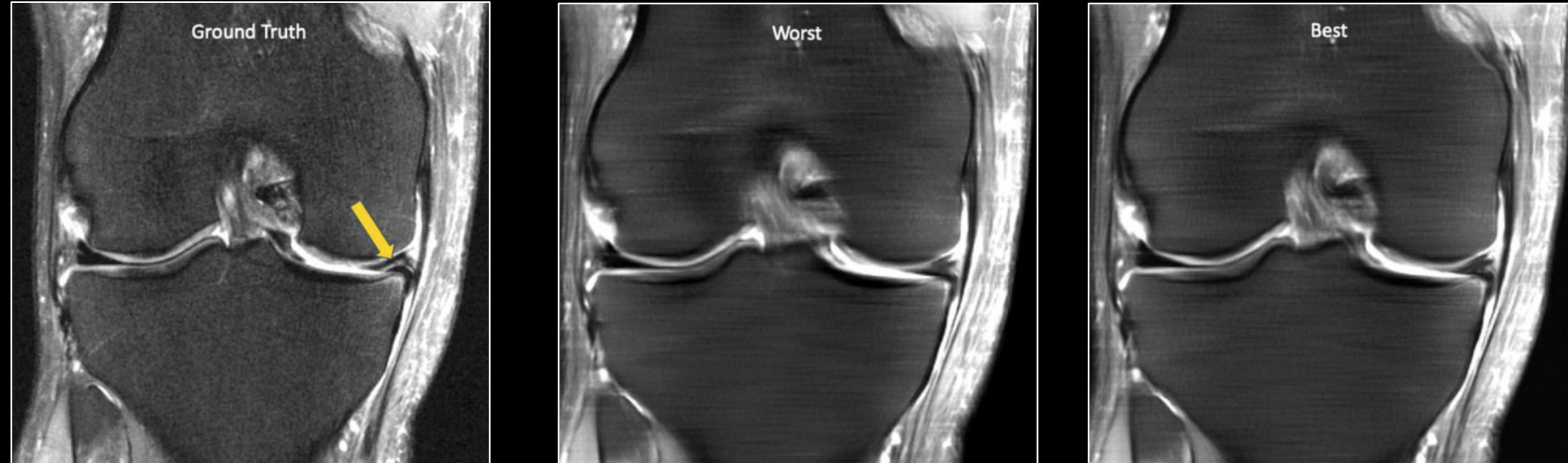
Under-sampled
k-space



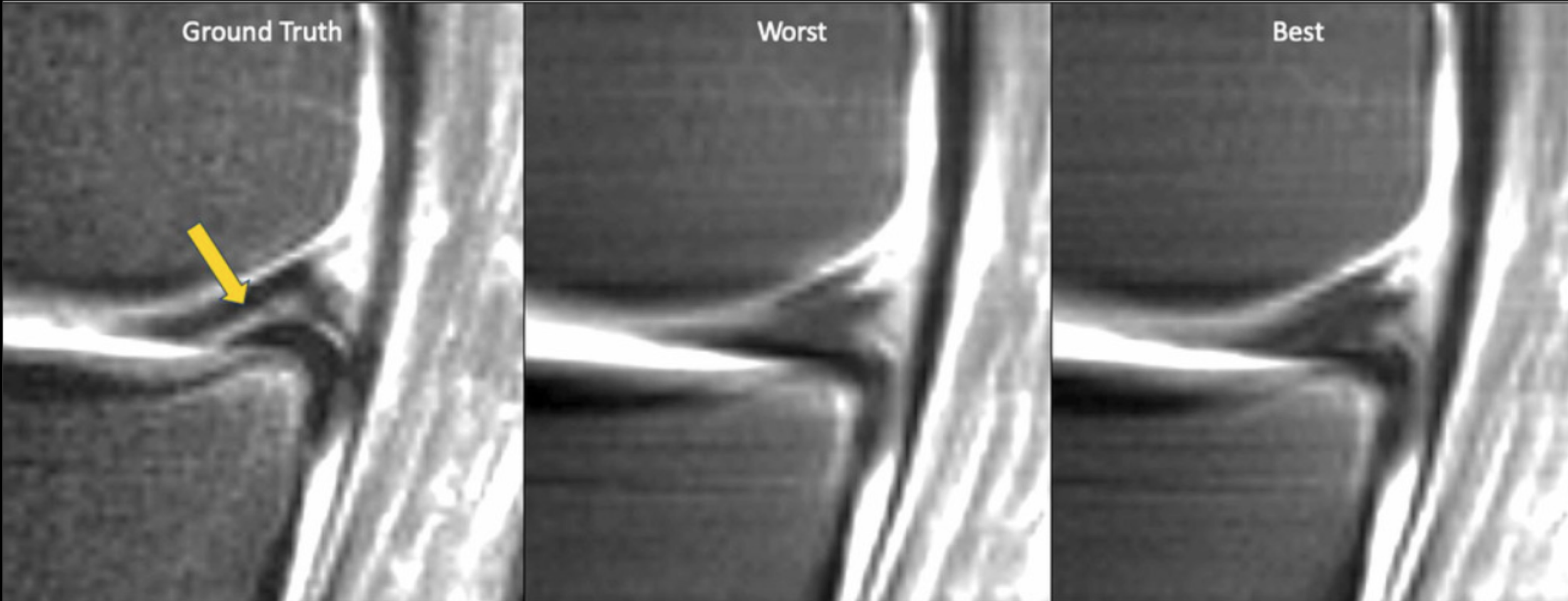
Methods



FastMRI results: loss of meniscal tear



The False Negative Phenomenon

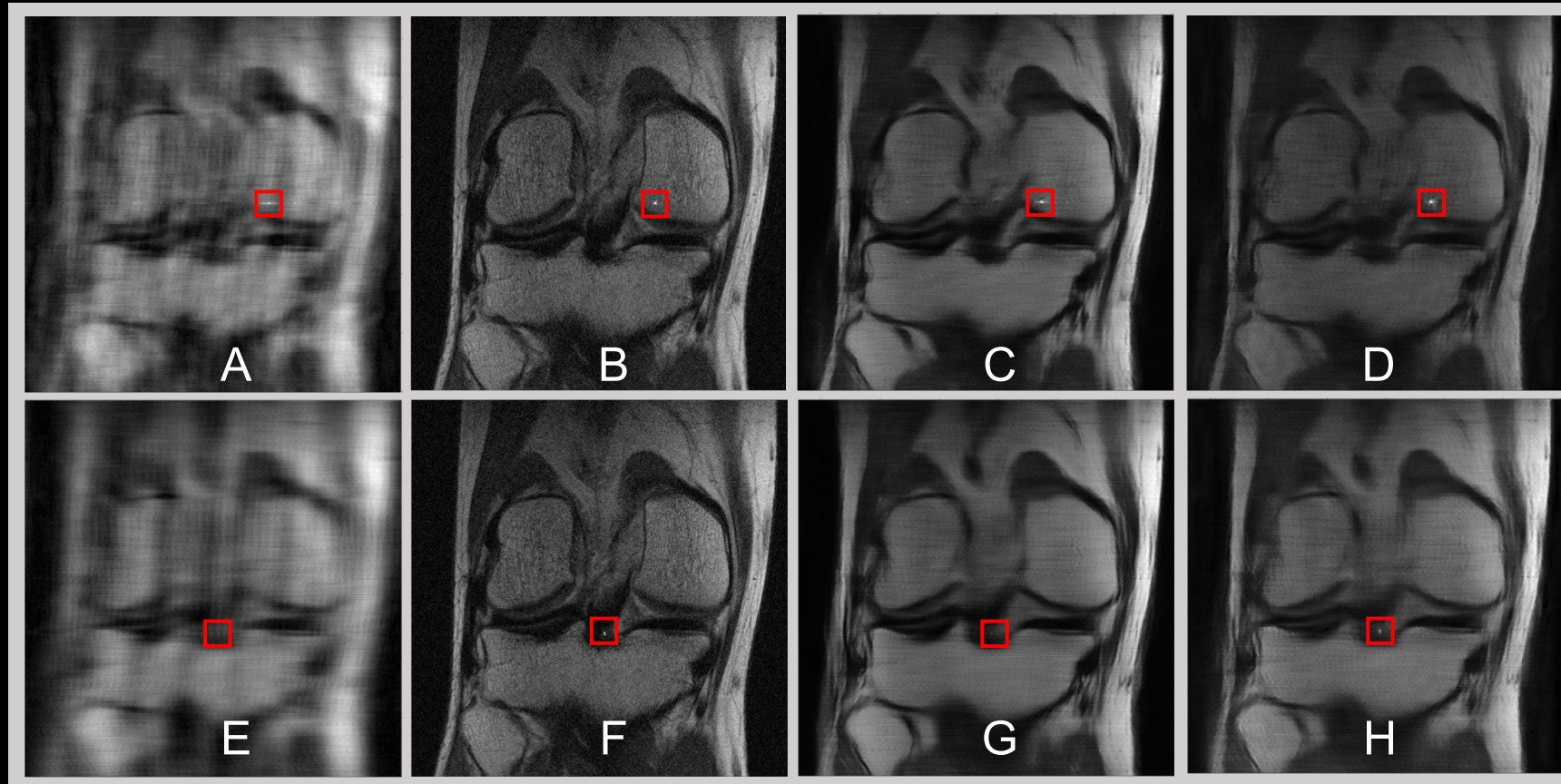


Two hypotheses for the false negative problem:

- 1) *The information of small abnormality features is completely lost through the under-sampling process*
- 2) *The information of small abnormality features is not completely lost. Instead, it is attenuated and laid in the tail-end of the task distribution, hence is rare*

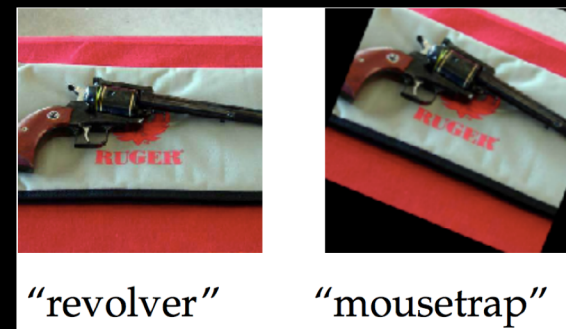
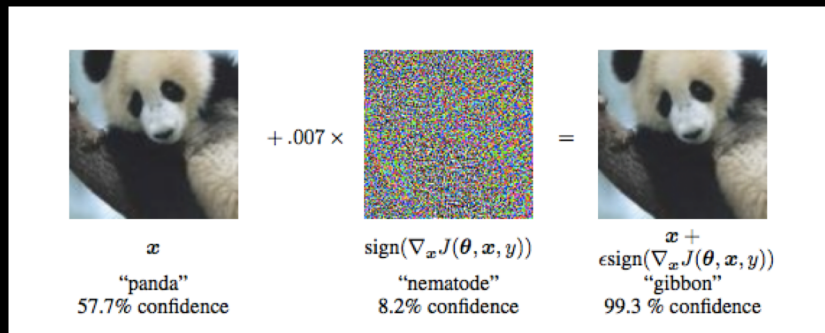
FNAF: false-negative adversarial feature

A perceptible small feature which is present in the ground truth MRI but has disappeared upon MRI reconstruction.

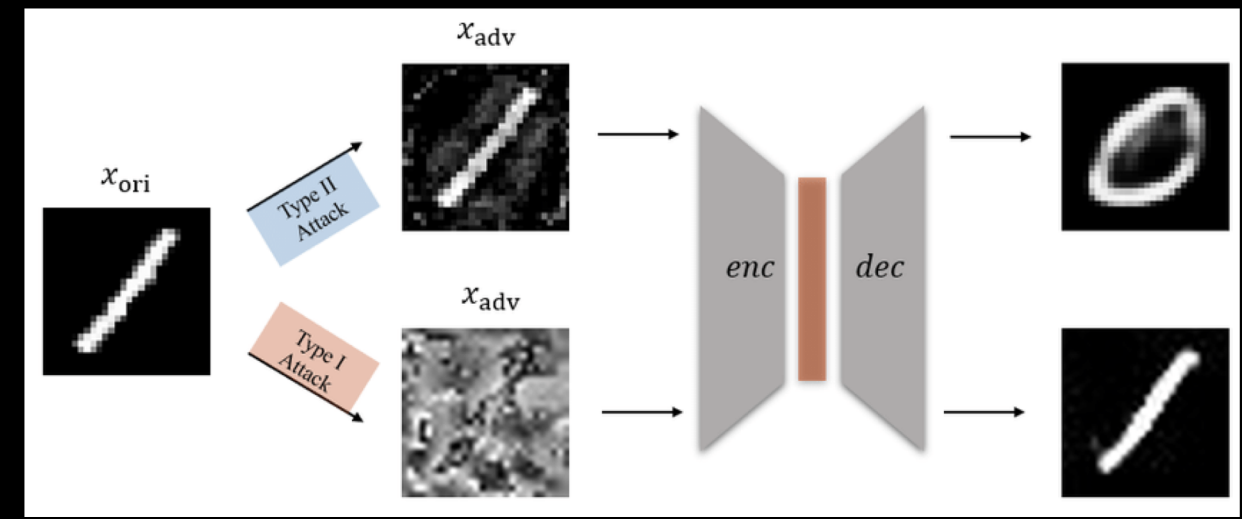
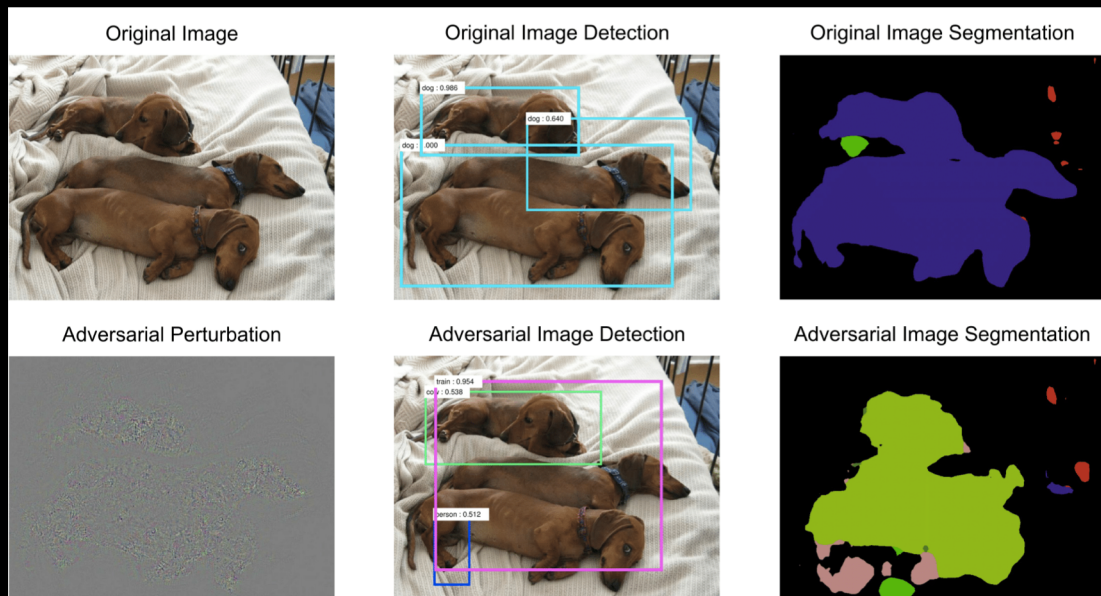


Adversarial Examples and Attacks

$$\max_{\delta \in S} L(\theta, x + \delta, y)$$

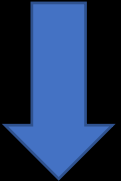


Adversarial Examples and Attacks



FNAF Attack

$$\max_{\delta \in S} L(\theta, x + \delta, y)]$$

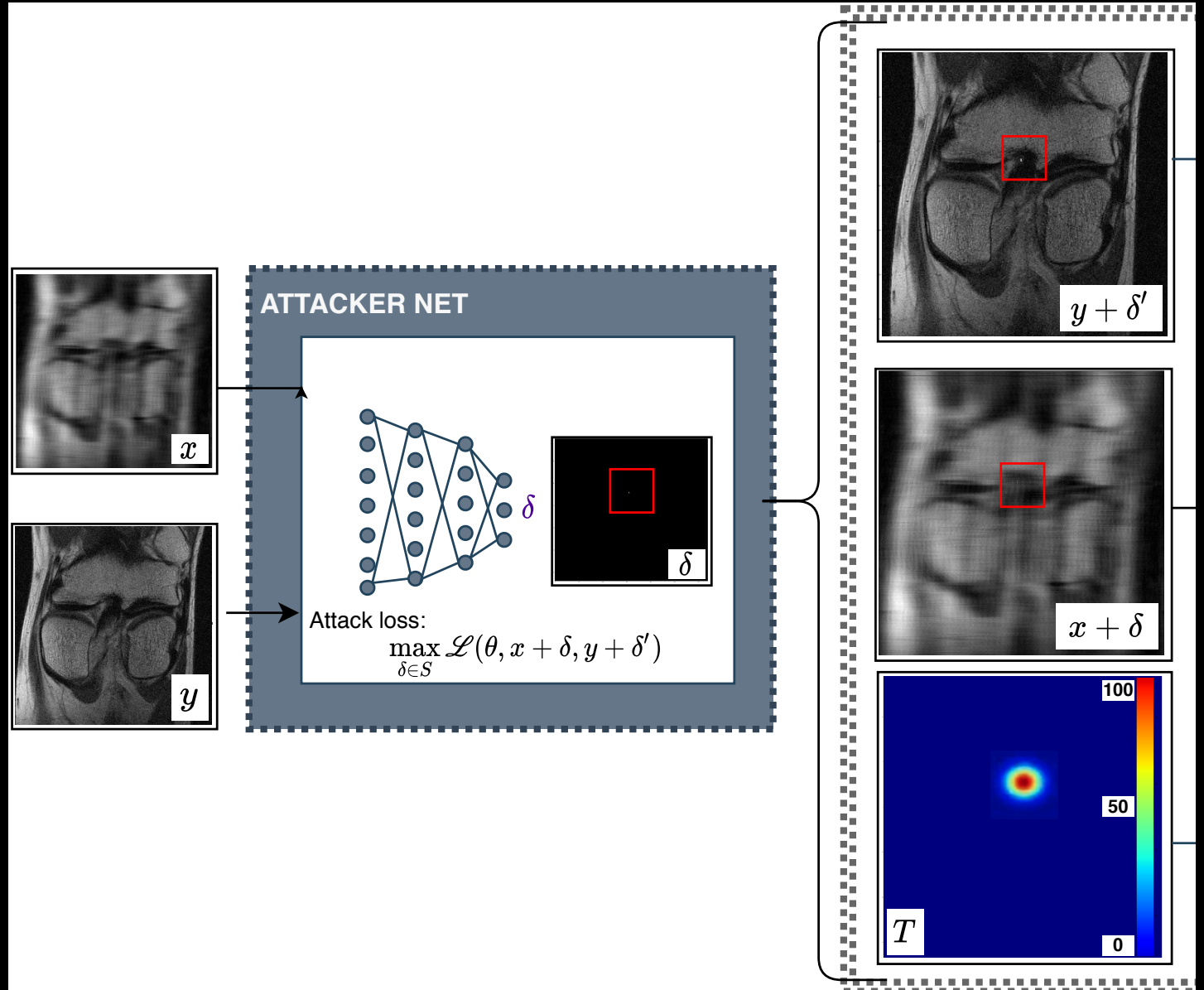


$$\max_{\delta \in S} L(\theta, x + \delta, y + \delta')]$$

$$\delta = U(\delta')$$

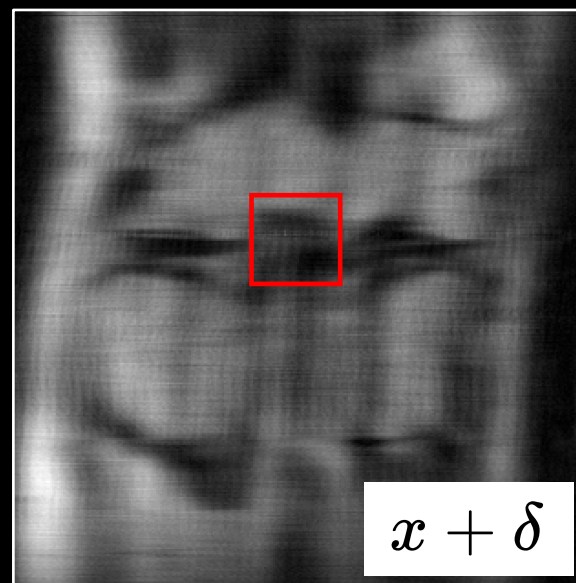
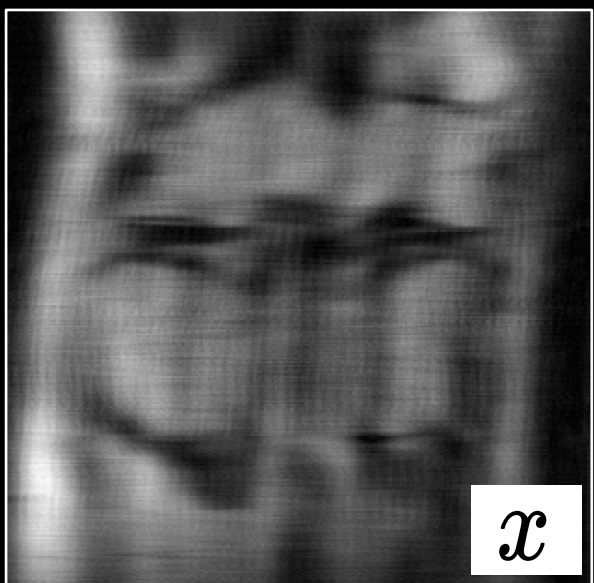
$$U(y) = \mathcal{F}^{-1}(M(\mathcal{F}(y)))$$

$$MSE(T(x), T(y))$$



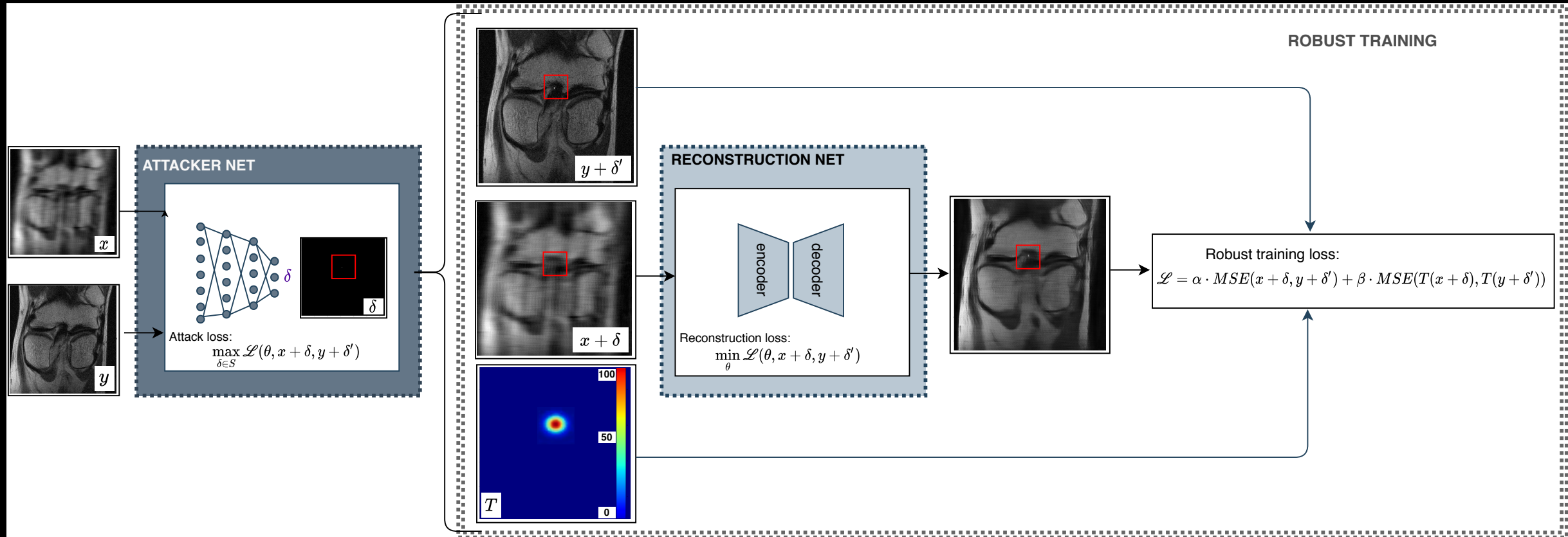
Under-sampling information preservation

$$D(x + \delta, x) > \varepsilon$$



Adversarial robustness training

$$\mathbb{E}_{(x,y) \sim D} [\max_{\delta \in S} L(\theta, x + \delta, y)]$$



Experimental Results

Table 1: Standard validation set evaluation with SSIM and normalized mean-square error (NMSE)

4×	SSIM	NMSE
U-Net	0.7213 ± 0.2621	0.03455 ± 0.05011
I-RIM	0.7501 ± 0.2546	0.03413 ± 0.05800
FNAF-robust U-Net	0.7197 ± 0.2613	0.03489 ± 0.05008

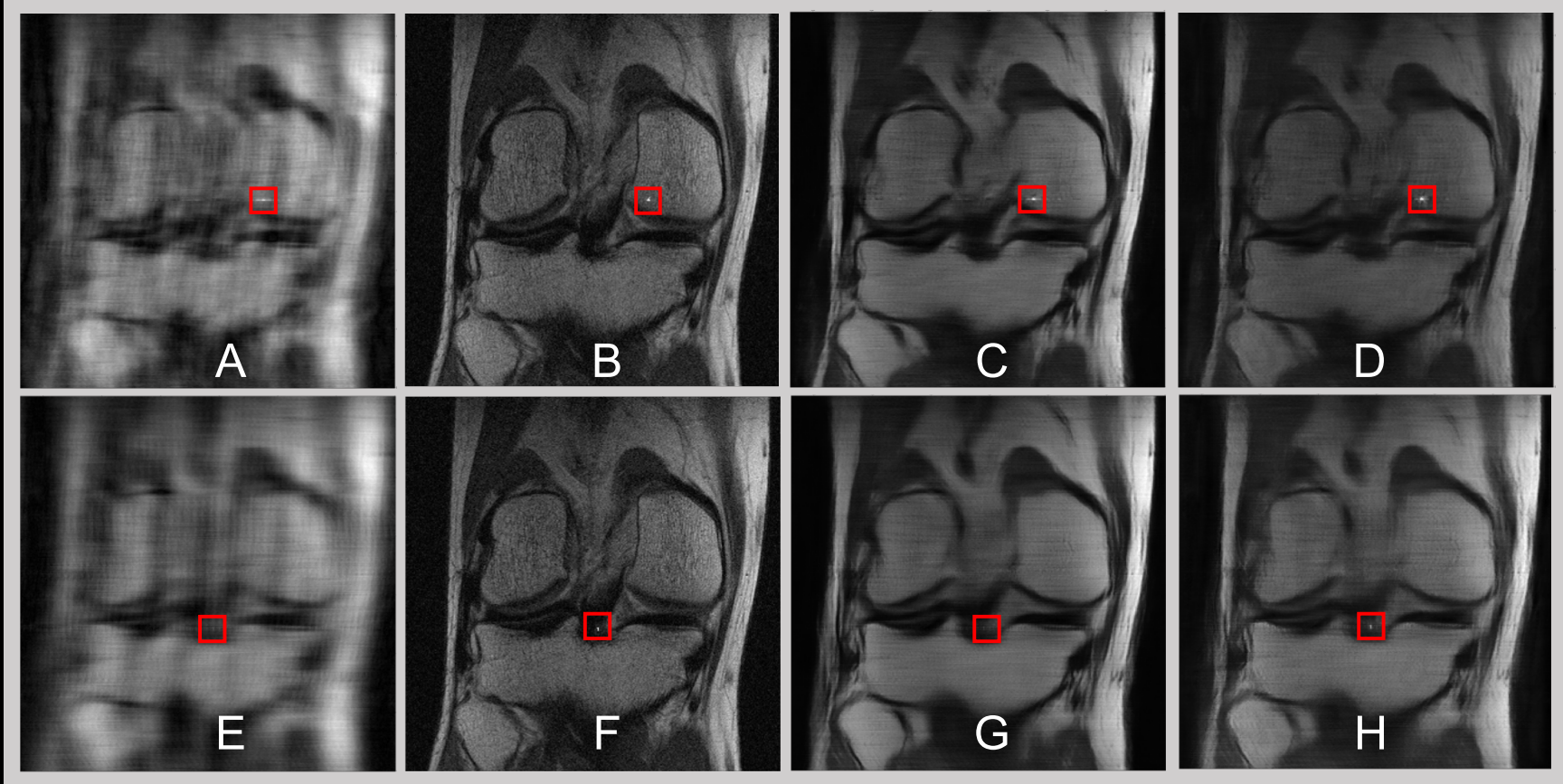
8×	SSIM	NMSE
U-Net	0.6548 ± 0.2942	0.04935 ± 0.04962
I-RIM	0.6916 ± 0.2941	0.04438 ± 0.06830
FNAF-robust U-Net	0.6533 ± 0.2924	0.04962 ± 0.05670

Table 2: FNAF attack evaluations.

4×	RS (Attack Rate %)	FD (Attack Rate %)	RS (MSE)	FD (MSE)
U-Net	84.44	72.17	0.001530	0.001386
I-RIM	44.49	34.60	0.001164	0.001080
FNAF-robust U-Net	12.71	10.48	0.000483	0.000466

8×	RS (Attack Rate %)	FD (Attack Rate %)	RS (MSE)	FD (MSE)
U-Net	86.00	74.84	0.001592	0.001457
I-RIM	77.39	63.88	0.001470	0.001349
FNAF-robust U-Net	15.09	13.30	0.000534	0.000467

Qualitative Results



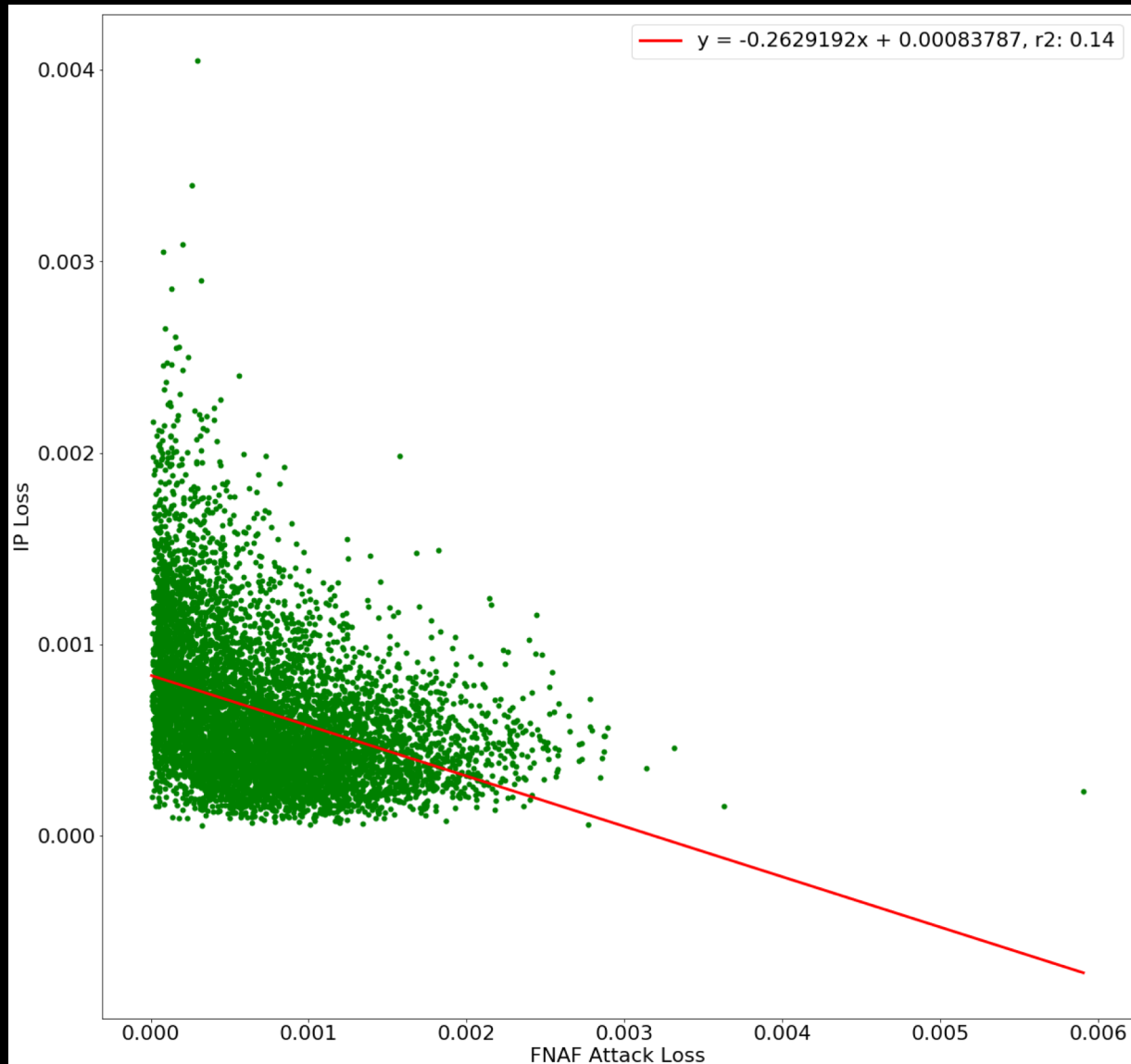
The top row (A-D) shows a "failed" FNAF attack. The bottom row (E-H) shows a "successful" FNAF attack. Column 1 contains the under-sampled zero-filled images. Column 2 contains the fully-sampled ground truth images. Column 3 contains U-Net reconstructed images. Column 4 contains FNAF-robust U-Net reconstructed images. (C-G-D-H) FNAF reconstruction: (C) adversarial loss of 0.000229. (G) adversarial loss of 0.00110. (D) adversarial loss of $9.73 \cdot 10^{-5}$. (H) adversarial loss of 0.000449

Information Preservation (IP)

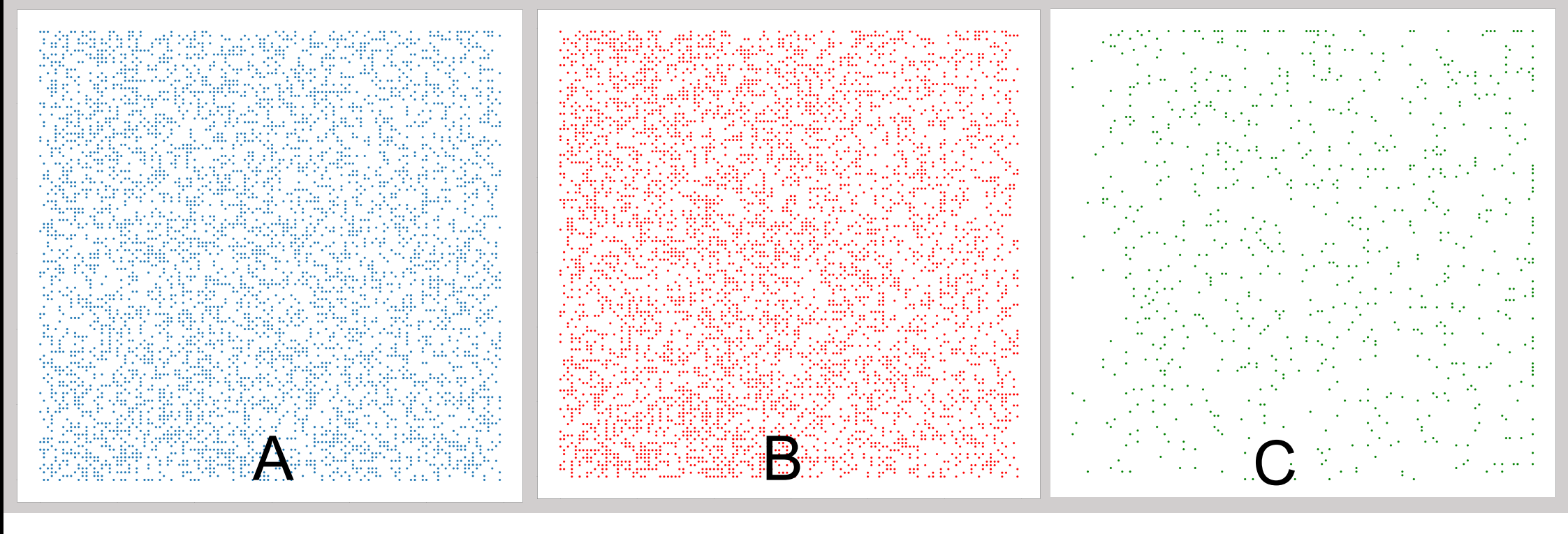
$$D(x + \delta, x) > \varepsilon$$

	Random	U-Net FNAF	I-RIM FNAF	Robust U-Net FNAF
Acceptance Rate (%)	99.82	99.72	99.76	99.34
IP Loss (MSE)	0.00064	0.00050	0.00051	0.00052

FNAF Attack Loss vs. IP Loss



FNAF Location Distribution and Transferability

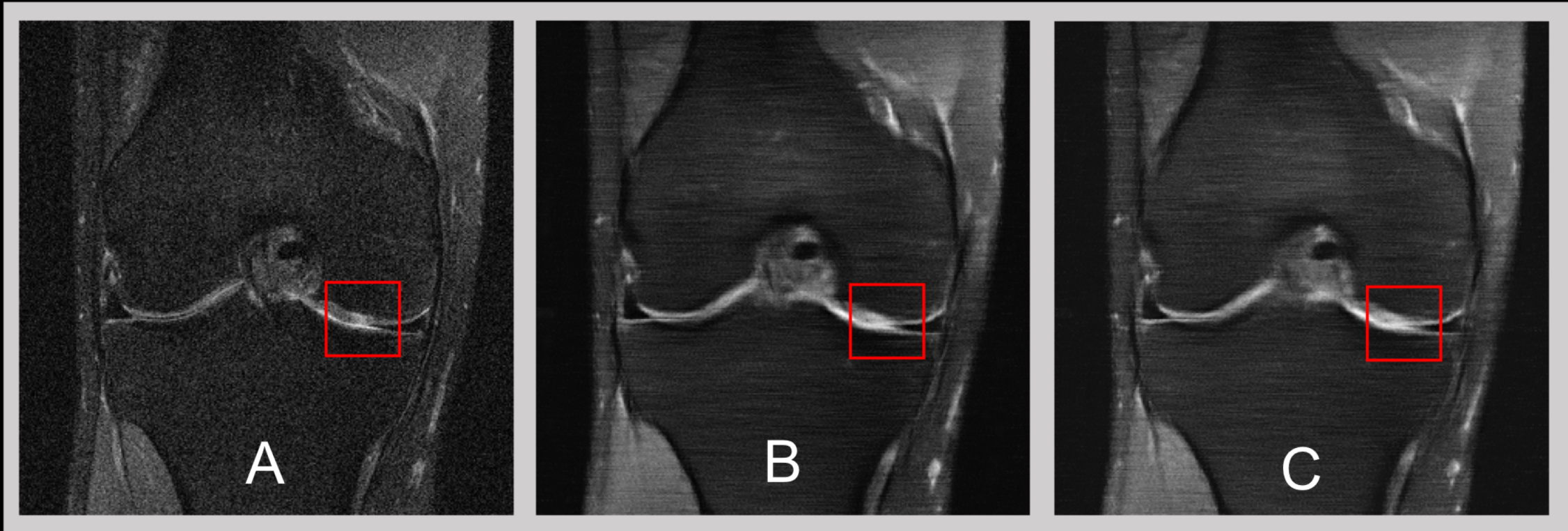


FNAF location distribution within the 120x120 center crop of the image of (A) U-Net, (B) I-RIM, (C) FNAF-robust U-Net

We take FNAF examples from U-Net and apply them to I-RIM, and observe a 89.48% attack rate.

Real-world Abnormalities reconstruction

	Cartilage Lesion Rate	Meniscus Lesion Rate
U-Net	1/8	8/9
FNAF-robust U-Net	3/8	9/9



(A) Ground truth: small cartilage lesion in femur. (B) U-Net: Area of cartilage lesion not defined and resembles increased signal intensity. (C) FNAF-robust U-Net: Cartilage lesion preserved but less clear.

Limitations

- *FNAF attack hit rate was defined heuristically*
- *Attack inner maximization optimization has no guarantee and can be expensive*
- *Adversarial training is only empirically robust*
- *Limited real world abnormalities evaluation*

Conclusions and Future directions

- Two hypotheses
 - 1) *The information of small abnormality features is completely lost through the under-sampling process*
 - 2) *The information of small abnormality features is not completely lost. Instead, it is attenuated and laid in the tail-end of the task distribution, hence is rare*
- Address our limitations
- Robustness in other medical imaging tasks

Acknowledgements

Valentina Pedoia's Lab

Francesco Calivà

Rutwik Shah

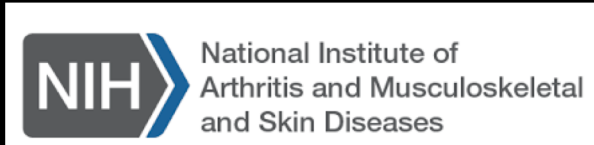
Sharmila Majumdar's Lab

Misung Han

Claudia Iriondo

Funding source

This project was supported by R00AR070902 (VP), R61AR073552 (SM/VP) from the National Institute of Arthritis and Musculoskeletal and Skin Diseases, National Institutes of Health, (NIH-NIAMS).



victorcheng21@berkeley.edu



Paper #28